Encapsulating Sub-Site Analogues of the [FeFe]-Hydrogenases in Micelles Enables Direct Water Interactions.

Robby Fritzsch,[1] Owen Brady,[1] Elaine Adair,[1] Joseph A. Wright,[2] Christopher J Pickett,[2] and Neil T. Hunt[1]*

1) Department of Physics, University of Strathclyde, SUPA, 107 Rottenrow East, Glasgow, UK

2) Energy Materials Laboratory, School of Chemistry, University of East Anglia, Norwich, NR4 7TJ, UK

AUTHOR INFORMATION

Corresponding Author

*neil.hunt@strath.ac.uk

ABSTRACT

Encapsulation of sub-site analogues of the [FeFe]-hydrogenase enzymes in supramolecular structures has been shown to dramatically increase their catalytic ability, but the molecular basis for this enhancement remains unclear. We report the results of experiments employing infrared absorption, ultrafast infrared pump-probe and 2D-IR spectroscopy to investigate the molecular environment of $Fe_2(pdt)(CO)_6$ (pdt: propanedithiolate) [**1**] encapsulated in the dispersed alkane phase of a heptane-dodecyltrimethylammonium bromide-water microemulsion. It is demonstrated that **1** is partitioned between two molecular environments, one that closely resembles bulk heptane solution and a second that features direct hydrogen-bonding interactions with water molecules that penetrate the surfactant shell. Our results demonstrate that the extent of water access to the normally water-insoluble sub-site analogue **1** can be tuned with micelle size, while IR spectroscopy provides a straightforward tool that can be used to measure and fine-tune the chemical environment of catalyst species in self-assembled structures.

TOC GRAPHICS

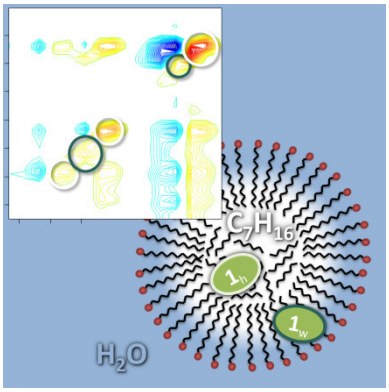

KEYWORDS [FeFe] hydrogenase; infrared spectroscopy, ultrafast infrared spectroscopy, micelle, water solubility

The ability of synthetic analogues of the active subsite of the [FeFe]-hydrogenase ([FeFe]-H_2ase) enzymes to catalyze the production of molecular hydrogen has generated considerable interest, owing to the belief that they could offer an economically-viable alternative to the rare-metal catalysts that are the current technological state-of-the-art.[1] A range of molecular architectures have been reported with varying catalytic abilities, but several challenges must be overcome before these systems can bridge the gap to technological applications.[2-6] In particular, even the most effective synthetic [FeFe]-H_2ase analogues are yet to match the efficiency of the natural enzyme, while the water insolubility and oxygen sensitivity of the analogues can also be prohibitive towards their development as robust fuel sources. Furthermore, in order to achieve catalytic turnover and the desirable light activated H_2 production from water, it is necessary to combine the sub-site analogue with a photosensitizer and sacrificial electron donor to create a functional system, although self-sensitizing systems have been reported recently. [7]

Encapsulation of [FeFe]-H_2ase subsite analogues in self-assembled or supramolecular systems has been shown to improve stability and lead to increases in catalytic efficiency.[8-12] Examples include the use of polymeric micelles to form 'microreactors',[8] encapsulation in gels or resins,[1,13] oligosaccharides[11] and dendrimers.[1] The reasons cited for the increased efficiency range from co-localization of the components to second coordination sphere H-bonding interactions with the sub-site analogue that resemble those of the natural enzyme. A factor that is likely to be equally significant, but not widely considered, is the ability of such structures to place the catalytic species in an environment where it is stably in contact with aqueous solution and so more readily accessible by the protons needed for the H_2 evolution reaction. This function is achieved by hydrophobic channels in the natural enzyme and must be replicated in any supramolecular or self-assembled system.

Infrared (IR) spectroscopy is a sensitive probe of both the structure and chemical environment of [FeFe]-H_2ase sub-site analogues.[14] Here, we employ IR absorption spectroscopy, ultrafast IR pump-probe and 2D-IR spectroscopy to evaluate the effect of encapsulating the [FeFe]-H_2ase subsite analogue $Fe_2(pdt)(CO)_6$ (pdt = propanedithiolate), **1**, in micelles formed by the surfactant dodecyltrimethyl ammonium bromide (DTAB) in water. These oil-in-water microemulsions, in which the dispersed phase is a solution of **1** in heptane, provide a model system with which to gauge the ability of water to penetrate self-assembled structures and so to provide an insight into the likely role of this behavior in enhancing the catalytic function of **1**. Our results show that, not only can micelles be used to enable water access to the catalytic centers, but that IR absorption spectroscopy is a simple and reliable tool to evaluate water access during the materials design process.

The IR spectrum of **1** in heptane solution displays five peaks attributable to CO ligand stretching vibrations at 2075, 2036, 2006, 1991 and 1982 cm^{-1}, in agreement with previous studies (Fig.1(a)).[15] This heptane solution formed the dispersed phase of heptane-DTAB-water microemulsions, as specified in Table 1, that have been shown to produce near spherical micelles with little or no inter-micelle interactions.[16-18] In all cases, there is estimated to be less than one molecule of **1** per micelle (Table 1).

Micelle encapsulation results in the formation of a shoulder on the low frequency side of the peaks at 2075 and 2036 cm^{-1} and a broad, featureless component in the region of the three closely-spaced peaks near 2006-1982 cm^{-1} (see arrows, Fig. 1(a)). It is noteworthy that a similar

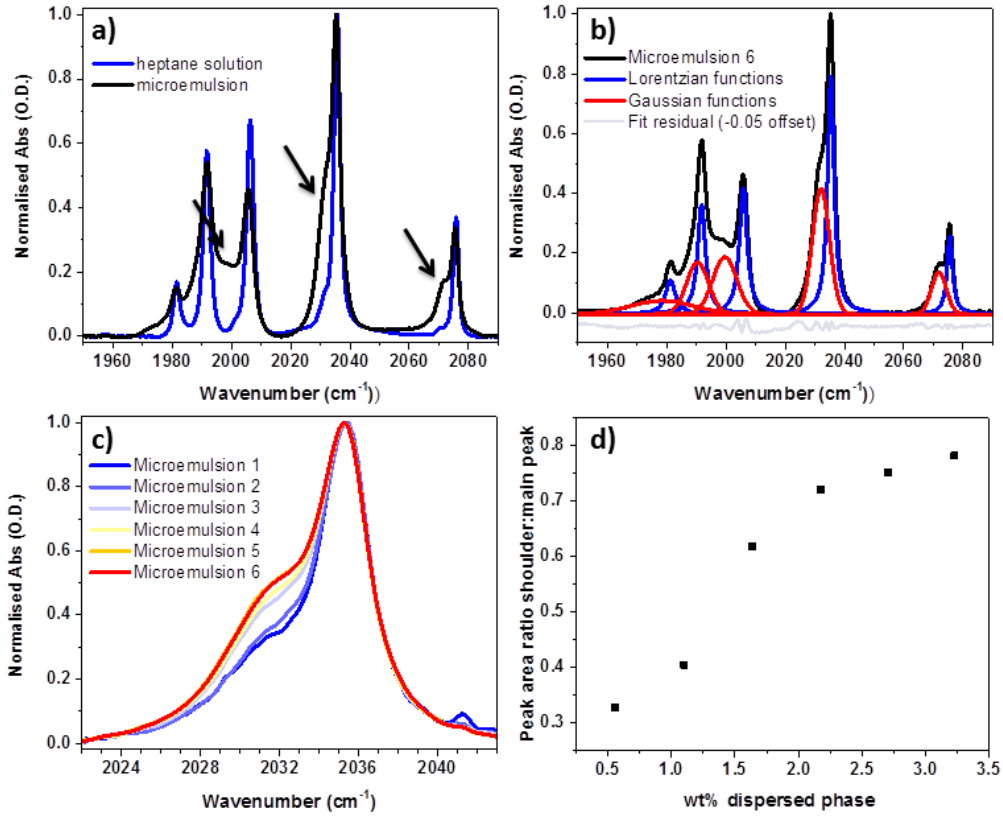

Figure 1: *(a) FT-IR spectra of* ***1*** *in heptane solution (blue) and encapsulated in microemulsion '6' (black, see Table 1 for sample details). Arrows mark the additional shoulders observed in the spectra of microemulsion samples. (b) Example of fit to microemulsion '6' FT-IR spectrum using sum of five Lorentzian (blue) and five Gaussian (red) lineshape functions. The fit residual is shown in light grey, offset slightly for visibility. Similar results were obtained for the other five microemulsion samples studied. A heptane solution of* ***1*** *required only the five Lorentzian functions to produce an accurate fit. (c) FT-IR spectra showing effect of increasing dispersed phase content of the microemulsion on the shoulder amplitude. This is also shown in (d) using the area ratio of the Gaussian (shoulder) to the Lorentzian (main peak) function for the 2036 cm*$^{-1}$ *peak.*

Sample	$V_{disp.\ phase}$ (µl)	wt % $_{disp.\ phase}$	$R_{micelle,\ est.}$ (nm)	n_1 (per micelle)	$n_{heptane}$ (per micelle)
1	8	0.55	1.64	0.03	4
2	16	1.10	1.67	0.07	8
3	24	1.64	1.70	0.10	12
4	32	2.17	1.73	0.13	17
5	40	2.70	1.75	0.17	21
6	48	3.23	1.78	0.20	25

Table 1: *Details of microemulsion samples discussed in text. Samples were made up by adding the required volume of a 55 mM stock solution of* ***1*** *in heptane ($V_{disp.\ phase}$) to a 20wt% DTAB/water-solution and allowing the mixture to equilibrate over 24h. This is also shown as a wt% of the dispersed phase. Estimates of the micellar radius ($R_{micelle,\ est}$) and the population numbers of* ***1*** *and heptane (n_1 and $n_{heptane}$ respectively) are based on an assumed surfactant aggregation number per micelle of 50 as per Ref* [18].

effect was also apparent in IR spectra of samples of **1** encapsulated in polymeric micelles that demonstrated enhanced catalytic activity, though this was not discussed in detail by the authors.[8]

Control experiments showed that **1** was insoluble in water in the absence of surfactant (as determined by the sensitivity limit of IR absorption spectroscopy), while inclusion of surfactant into heptane solutions of **1** had no impact upon the IR spectrum. Adding **1** to samples featuring a 50:50 v/v mixture of water and heptane produced a biphasic system in which the IR spectrum of **1** could only be detected in the heptane layer. This spectrum exactly matched that observed in pure heptane solution. These experiments confirm that the new features apparent in the IR

spectrum of **1** are due to micelle encapsulation within an aqueous continuous phase and are not due to water saturation of the heptane phase.

Lineshape fitting of the IR absorption spectra showed that the spectrum of **1** in heptane solution is well-represented by five Lorentzian lineshapes corresponding to each of the CO stretching vibrational modes. To obtain the same quality of fit to the IR spectra of the microemulsion samples these Lorentzian peaks had to be augmented by five additional Gaussian lineshapes, each broader (~7 *vs* ~2.5 cm^{-1} FWHM) and shifted to the low frequency relative to the corresponding Lorentzian (Fig 1(b)). The quality of fit obtained using this approach could not be improved by the use of more complex Voigt profiles. Increasing the quantity of dispersed phase added to the microemulsion to swell the micelle size (Table 1) resulted in a progressive increase in the amplitude of the shoulder relative to the main peak. This continued up to a dispersed phase content of 2 wt% where a plateau was reached (Fig.1(c)). By contrast, increasing the concentration of **1** for constant volume of dispersed phase had no effect on the spectrum of **1**.

Ultrafast IR pump-probe experiments were carried out on the heptane solution and two representative microemulsion samples (Samples '3' and '6' from Table 1), chosen to provide a change in micelle size for a given dispersed phase concentration of **1**. The pump-probe spectra of the heptane solution exhibited peaks assignable to bleaches (negative) and transient absorptions (positive) originating from the v=0-1 and v=1-2 transitions of the CO stretching vibrations of **1** respectively (Fig. 2(a)), in good agreement with prior publications.[15] The spectra of both microemulsion samples were broadly similar, though with noticeable broadening to the low frequency side of the peaks consistent with the shoulders observed in the absorption spectra.

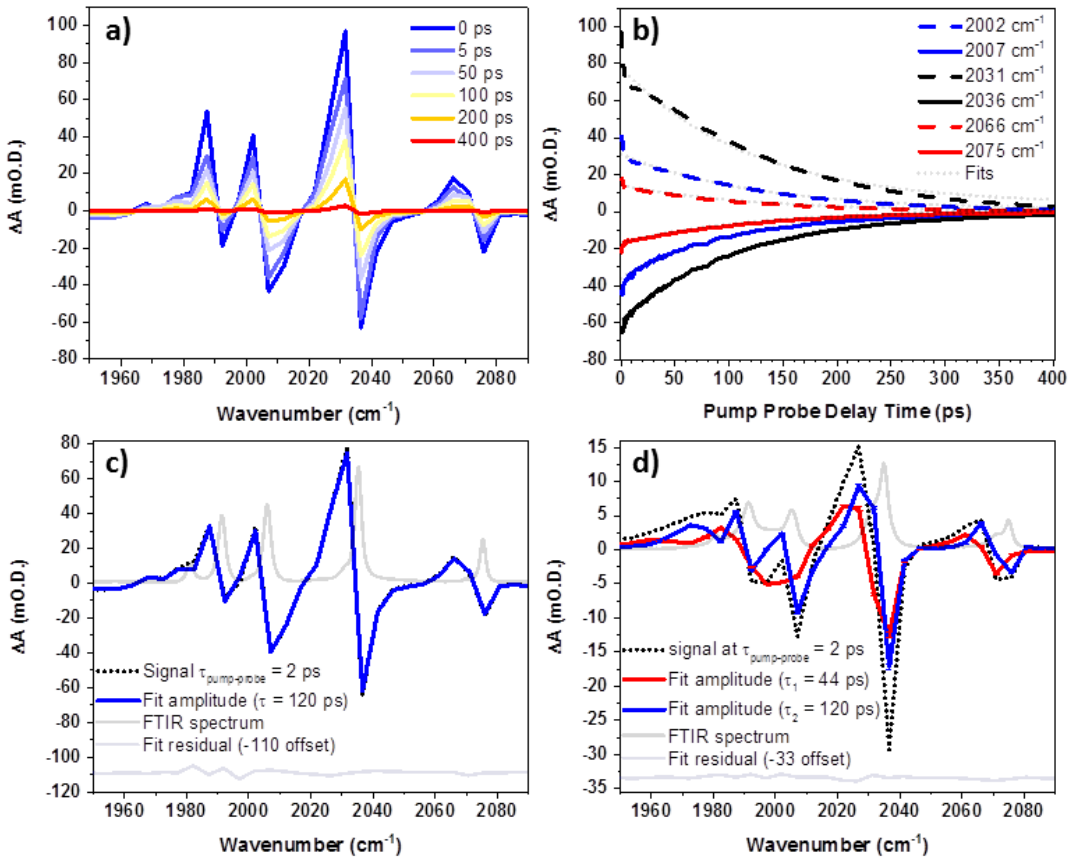

Figure 2: *(a) Representative IR pump-probe spectra of* ***1*** *encapsulated in heptane at a range of pump-probe delay times, as shown in the figure legend. (b) Temporal decay of peak amplitudes taken from (a) with fits to exponential functions shown in grey. The legend identifies specific peaks in the spectrum by frequency. (c) Example of fitting IR pump-probe spectrum of* ***1*** *in heptane solution to a single exponential function. Experimental data (black dotted line) is compared with the fit result showing the amplitude of a single exponential decay function with a decay timescale of 120 ps (blue line). The FT-IR spectrum is shown for comparison (dk grey). The fit residual is shown (lt grey) but offset for clarity. (d) Results of fitting the IR pump-probe spectrum of microemulsion '6' to a bi-exponential function, showing the amplitudes of the 44 ps (red) and 120 ps (blue) components. The fit residual is shown (lt grey) but offset for clarity. Similar results were obtained for microemulsion '3'.*

Global fitting of the temporal dynamics of the pump-probe data to both single and bi-exponential functions was used to quantify the vibrational relaxation dynamics of the modes of **1**. In both heptane solution and the microemulsion samples, a very fast decay component was observed on sub-ps timescales that was attributed to the instrument response and so fitting was started at a pump-probe delay of 2 ps (Fig 2(b)). For the heptane solution, the data were well-represented by a single decay timescale of 120 ps, the amplitude of which closely matched the peaks in the pump-probe spectra (Fig.2(c)). This agrees well with previous reports of the vibrational lifetime of the carbonyl modes of **1** in alkane solution showing that all modes relax with a similar vibrational lifetime. [15]

By contrast, a bi-exponential function was required to adequately represent the microemulsion data, returning decay timescales of 44 and 120 ps irrespective of micelle size (Fig. 2(d)). Applying a bi-exponential fit to the heptane solution data led to a collapse of this function to a single exponential result. Examination of the amplitudes of the two components in the microemulsion data showed that the 120 ps decay timescale corresponds to the peaks observed in the heptane spectrum, while the 44 ps lifetime is primarily associated with the shoulders and the broad feature that are exclusive to the encapsulated system (Fig 2(d)). The relative amplitude of the 44 ps component was found to increase slightly with increased micelle size, but pump-probe experiments are less sensitive than IR absorption and the change in amplitude of the 44 ps component was comparable to the anticipated error in the measurement.

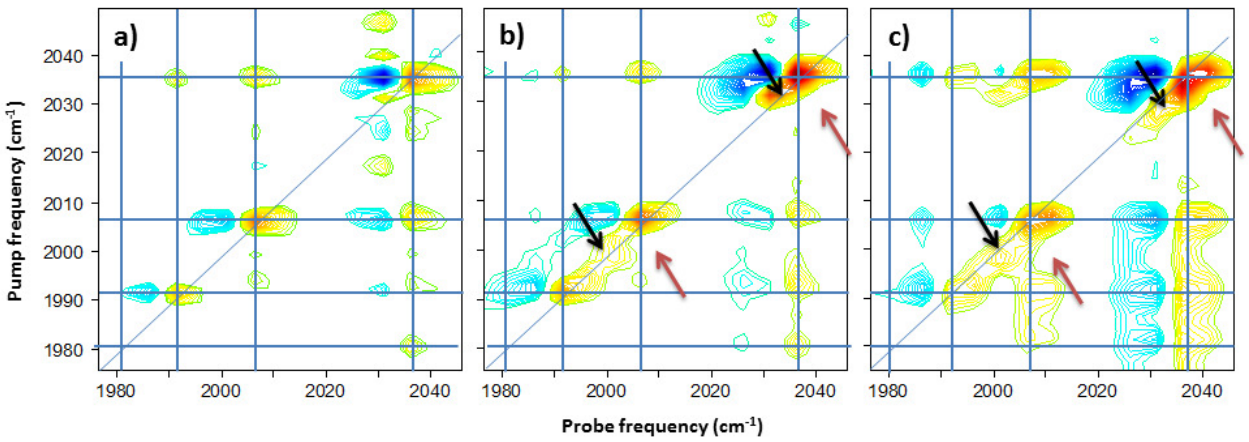

Figure 3: *2D-IR spectra of (a)* ***1*** *in heptane solution at a waiting time of 5 ps. The region between 1980 and 2050 cm^{-1} is shown for clarity. Blue lines show position of peaks in IR absorption spectra. (b&c) 2D-IR spectra of* ***1*** *encapsulated in microemulsion '6' at waiting times of (b) 5 ps and (c) 20 ps. The colour scale runs from negative (red) to positive (blue). Black arrows show the additional diagonal features arising from microemulsion encapsulation. Red arrows show the absence of off-diagonal peaks that would indicate coupling or chemical exchange between the main diagonal lineshape and shoulder.*

2D-IR spectroscopy of the heptane solution revealed diagonal peaks corresponding to each of the bands in the IR absorption spectrum of **1** that were linked by off-diagonal peaks (Fig. 3). This is consistent with observations that the CO-stretching modes of **1** are vibrationally coupled. [15] Spectra obtained on microemulsion '6' were similar, but the circular diagonal peak shapes of the heptane spectra are augmented by diagonally-elongated features, which correspond exactly to the shoulders observed in the IR absorption spectrum (see black arrows, Fig. 3). Experiments on other microemulsion samples produced similar results, but returned a lower signal to noise ratio. Experiments as a function of 2D-IR waiting time showed that these shoulders evolve slightly over the first 20 ps of the waiting time to a somewhat more circular shape. This can be seen in

Fig. 3 as a slight broadening of the shoulder signals in the antidiagonal direction between waiting times of 5 and 20 ps. This behavior is consistent with spectral diffusion of an inhomogeneously-broadened lineshape, but the amplitude of the signal was too small to quantify the dynamics reliably.[19-21] Importantly, no off-diagonal peaks linking the shoulder to the main feature were observed (see red arrows, Fig. 3), which rules out the presence of either vibrational coupling or fast chemical exchange linking the two signals. [22]

Taken together, this data shows that the microemulsion gives rise to two sets of peaks in the IR spectrum of **1**, which correspond to two different chemical environments. One is spectroscopically indistinguishable from that of **1** in heptane solution and, depending on the wt% of the dispersed phase present, accounts for between half and four-fifths of the molecules of **1** (Fig 1(d)). The remaining fraction occupies a second environment that is unique to the micellar system, exhibiting a similar overall peak pattern to the heptane-like environment, but with broadened and red-shifted absorption bands and a shorter vibrational lifetime. The absence of coupling or fast exchange of **1** between the two environments suggests that they are chemically distinct.

The broadly similar spectral patterns observed in the two environments are not consistent with an alteration of the molecular structure of **1**. A change in electron density on the Fe centers could lead to a shift of the peaks of **1** to lower frequency, but no change in the oxidation state of **1** is expected from this experiment and this would be unlikely to significantly influence the vibrational relaxation dynamics of the modes. A uniform shift to lower frequency is consistent with a solvent-solute interaction, particularly in hydrogen bonding solvents. This could occur if **1** were located towards the edge of the micelle where water molecules might penetrate the long

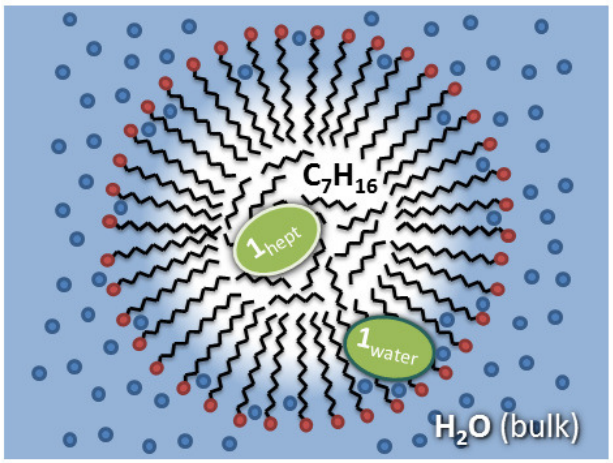

Figure 4: *Schematic diagram of the micellar environment based on IR spectroscopy studies. A central core of heptane-like solution is surrounded by a region in which water molecules penetrate the surfactant chains. Our data suggests that* ***1*** *is partitioned between these two environments as shown.*

alkyl chains of the surfactant molecules to some extent (Fig. 4), with the heptane-like environment experienced if **1** is located in the center of a micelle. Presumably, this environment will arise from a combination of dispersed-phase heptane and the long alkyl chains of the surfactant as the inclusion numbers of heptane molecules is still relatively low (Table 1).

Consistent with this model, it has been shown that the vibrational lifetime of CO ligand vibrations of water-soluble metallocarbonyls is much shorter than in alkane solvents; values of a few ps being reported for CO-releasing molecules (CORMs) in water. [23] The reduction in lifetime observed for the shoulder signals is not on this scale but a reduction by nearly two-thirds suggests a significant change in molecular environment. Indeed this is consistent with comparisons of [FeFe]-H_2ase analogues in non-polar and protic organic solvents, which indicated red-shift of the absorption peaks and a shortened vibrational lifetime in H-bonding

solvents. [24] It is noteworthy that the vibrational lifetime of **1** in the polar organic solvent acetonitrile showed little variation from that in heptane (~110 ps), which would seem to exclude any effect of the surfactant head group in accelerating vibrational relaxation.[15] The mechanism for enhanced vibrational relaxation in water is known to arise from spectral overlap of the CO stretching modes with the bend-libration combination band of water leading to efficient energy transfer and so water access to **1** in the micelle could give rise to both H-bonding interactions and a viable route to shortening the vibrational relaxation time. [23,25-27] This assignment would also give rise to the inhomogeneous broadening shown by the diagonal peaks in the 2D-IR spectra and the Gaussian, rather than Lorentzian, representation of the shoulders in the IR absorption data.

It is clear that the new environment does not completely resemble bulk aqueous solution. The diagonal peaks lack the fast spectral diffusion that is synonymous with bulk water, which would lead to the 2D-IR diagonal peak evolving from diagonally-elongated to circular on sub-ps timescales. While the shoulder peaks in the 2D-IR data do show some spectral diffusion, it is on timescales much slower than that of bulk water. [28-32]

Experiments measuring molecular dynamics within micelles have mainly focused on an aqueous dispersed phase, but they indicate that a core-shell type dynamic structure exists within the micelle. Molecules encapsulated within large micelles display dynamics that closely resemble the bulk solution phase of the dispersed species while smaller micelles show slower dynamics suggesting a restricted dynamic environment that is attributed to interaction of the dispersed phase with the surfactant shell of the micelles. Intermediate size micelles show dynamics that are a linear combination of these two environments. [33-35] The results for encapsulated **1** here suggest that they are consistent with **1** being partitioned between two

environments, with the slower spectral diffusion resulting from restricted motion of water that is encroaching between the surfactant chains. The lack of exchange of **1** between the two environments on the 20 ps timescales accessible suggests that this restricted molecular motion extends to **1** throughout the micelle also. It is plausible that this situation could be modified in larger micelles or other self-assembled systems that give rise to greater inhomogeneity in the range of environments accessible to the catalyst and so the observation of more complex dynamics.

This scenario is also consistent with measurements of CS_2 encapsulated in DTAB-water micelles using Optical Kerr Effect spectroscopy, which revealed a complex set of environments for the small CS_2 molecules created by folding of the long DTAB alkyl chains. CS_2 is larger than water and so if the former can penetrate the surfactant shell then it would be expected that water can also. [18] Similar regions of water penetration have also been proposed for channels within a phospholipid bilayer. [36,37]

In conclusion, we show that, as well as co-localization of reactants, encapsulating [FeFe]-H_2ase subsite analogues in a micelle environment within a continuous water phase enables water access to a significant fraction (up to 40%) of the encapsulated molecules. This effect is likely to contribute to reports of acceleration the catalytic rates of such systems by providing an access route for reactants. We show that the extent of water access is tuned by increasing the micelle size, presumably concomitant with a reduction in surfactant packing. This provides scope to control of the water content of the chemical environment of the catalyst via self-assembled systems. Furthermore, we demonstrate that IR spectroscopy is a useful and straightforward diagnostic tool for measuring this water access when designing complex molecular systems.

Materials and Methods:

Samples were made up as outlined in Table 1 by adding the desired amount of a 55mM stock solution of **1** in heptane to a 20wt% DTAB/water-solution and allowing the mixture to equilibrate over 24hrs. The result was a clear, single phase microemulsion sample consistent with previous work.[18]

For all IR measurements, the sample was held between two CaF_2 windows separated by a 50 μm thickness poly-tetrafluoroethylene spacer. IR absorption spectra were obtained using a Bruker Vertex 70 Fourier-transform IR instrument. Ultrafast 2D-IR spectra were obtained using the Strathclyde spectrometer employing the pseudo pump-probe geometry Fourier Transform method described previously. [38] Ultrafast IR laser pulses (~ 200 fs duration) were produced by a regeneratively-amplified Ti:sapphire laser system (1 kHz, 3 mJ), pumping an optical parametric amplifier (OPA) equipped with difference frequency mixing of the signal and idler outputs. The resulting mid-IR pulses (5 μm center wavelength, ~300 cm^{-1} bandwidth) are split into pump (95% intensity) and probe (5%) beams. The pump beam is routed into an interferometer to generate the two excitation pulses separated by the coherence time (τ) while an additional optical delay stage is used to set the waiting time (T_w) between pump and probe pulses. Scanning τ for fixed T_w allows the 2D-IR spectrum to be obtained by dispersing the signal in a spectrometer and detecting with a 64-element HgCdTe array detector. Fourier transformation along τ provides the pump axis of the spectrum. IR pump-probe data were obtained using the same apparatus but employing only one pump pulse. 'Magic-angle' polarization of pump and probe was used to negate the effect of molecular rotation on the signal decay dynamics.

AUTHOR INFORMATION

The authors declare no competing financial interests.

REFERENCES

(1) Simmons, T. R.; Berggren, G.; Bacchi, M.; Fontecave, M.; Artero, V. Mimicking hydrogenases: From Biomimetics to Artificial Enzymes; *Coord Chem Rev* **2014**, *270*, 127-150

(2) Tard, C.; Pickett, C. J. Structural and Functional Analogues of the Active Sites of the [Fe]-, [NiFe]-, and [FeFe]-Hydrogenases; *Chemical Reviews* **2009**, *109*, 2245-2274

(3) Liu, X. M.; Ibrahim, S. K.; Tard, C.; Pickett, C. J. Iron-only Hydrogenase: Synthetic, Structural and Reactivity Studies of Model Compounds; *Coord Chem Rev* **2005**, *249*, 1641-1652

(4) Tschierlei, S.; Ott, S.; Lomoth, R. Spectroscopically Characterized Intermediates of Catalytic H_2 Formation by FeFe Hydrogenase Models; *Energy & Environmental Science* **2011**, *4*, 2340-2352

(5) Mulder, D. W.; Shepard, E. M.; Meuser, J. E.; Joshi, N.; King, P. W.; Posewitz, M. C.; Broderick, J. B.; Peters, J. W. Insights into FeFe-Hydrogenase Structure, Mechanism, and Maturation; *Structure* **2011**, *19*, 1038-1052

(6) Gloaguen, F.; Rauchfuss, T. B. Small Molecule Mimics of Hydrogenases: Hydrides and Redox; *Chem Soc Rev* **2009**, *38*, 100-108

(7) Wang, W.; Rauchfuss, T. B.; Bertini, L.; Zampella, G. Unsensitized Photochemical Hydrogen Production Catalyzed by Diiron Hydrides; *J Am Chem Soc* **2012**, *134*, 4525-4528

(8) Wang, F.; Wen, M.; Feng, K.; Liang, W.-J.; Li, X.-B.; Chen, B.; Tung, C.-H.; Wu, L.-Z. Amphiphilic Polymeric Micelles as Microreactors: Improving the Photocatalytic Hydrogen

Production of the FeFe-Hydrogenase Mimic in Water; *Chemical Communications* **2016**, *52*, 457-460

(9) Hansen, M.; Troppmann, S.; Koenig, B. Artificial Photosynthesis at Dynamic Self-Assembled Interfaces in Water; *Chemistry-a European Journal* **2016**, *22*, 58-72

(10) Wu, L.-Z.; Chen, B.; Li, Z.-J.; Tung, C.-H. Enhancement of the Efficiency of Photocatalytic Reduction of Protons to Hydrogen via Molecular Assembly; *Accts Chem Res* **2014**, *47*, 2177-2185

(11) Jian, J.-X.; Liu, Q.; Li, Z.-J.; Wang, F.; Li, X.-B.; Li, C.-B.; Liu, B.; Meng, Q.-Y.; Chen, B.; Feng, K.; Tung, C.-H.; Wu, L.-Z. Chitosan Confinement Enhances Hydrogen Photogeneration from a Mimic of the Diiron Subsite of FeFe-Hydrogenase; *Nature Communications* **2013**, *4*, Art No. 2695

(12) Wang, H.-Y.; Wang, W.-G.; Si, G.; Wang, F.; Tung, C.-H.; Wu, L.-Z. Photocatalytic Hydrogen Evolution from Rhenium(I) Complexes to FeFe Hydrogenase Mimics in Aqueous SDS Micellar Systems: A Biomimetic Pathway; *Langmuir* **2010**, *26*, 9766-9771

(13) Frederix, P. W. J. M.; Kania, R.; Wright, J. A.; Lamprou, D. A.; Ulijn, R. V.; Pickett, C. J.; Hunt, N. T. Encapsulating [FeFe]-Hydrogenase Model Compounds in Peptide Hydrogels Modifies Stability and Photochemistry; *Dalton Trans* **2012**, *41*, 13112-13119

(14) Hunt, N. T.; Wright, J. A.; Pickett, C. Detection of Transient Intermediates Generated from Subsite Analogues of FeFe Hydrogenases; *Inorg Chem* **2016**, *55*, 399-410

(15) Stewart, A. I.; Clark, I. P.; Towrie, M.; Ibrahim, S.; Parker, A. W.; Pickett, C. J.; Hunt, N. T. Structure and Vibrational Dynamics of Model Compounds of the [FeFe]-Hydrogenase

Enzyme System via Ultrafast Two-Dimensional Infrared Spectroscopy; *J Phys Chem B* **2008**, *112*, 10023-10032

(16) Jaye, A. A.; Hunt, N. T.; Meech, S. R. Ultrafast Dynamics in the Dispersed Phase of Oil-in-Water Microemulsions: Monosubstituted Benzenes Incorporated into Dodecyltrimethylammonium bromide (DTAB) Aqueous Micelles; *Langmuir* **2005**, *21*, 1238-1243

(17) Hunt, N. T.; Jaye, A. A.; Hellman, A.; Meech, S. R. Ultrafast Dynamics of Styrene Microemulsions, Polystyrene Nanolatexes, and Structural Analogues of Polystyrene; *J Phys Chem B* **2004**, *108*, 100-108

(18) Hunt, N. T.; Jaye, A. A.; Meech, S. R. Ultrafast Dynamics in Microemulsions: Optical Kerr Effect Study of the Dispersed Oil Phase in a Carbon Disulride-Dodecyltrimethylammonium Bromide-Water Microemulsion; *J Phys Chem B* **2003**, *107*, 3405-3418

(19) Park, S.; Fayer, M. D. Hydrogen Bond Dynamics in Aqueous NaBr Solutions; *Proc Nat Acad Sci* **2007**, *104*, 16731-16738

(20) Kwak, K.; Park, S.; Finkelstein, I. J.; Fayer, M. D. Frequency-Frequency Correlation Functions and Apodization in Two-Dimensional Infrared Vibrational Echo Spectroscopy: A New Approach; *J Chem Phys* **2007**, *127*, 124503

(21) Roberts, S. T.; Loparo, J. J.; Tokmakoff, A. Characterization of Spectral Diffusion from Two-Dimensional Line Shapes; *J Chem Phys* **2006**, *125*, 084502

(22) Kwak, K.; Zheng, J. R.; Cang, H.; Fayer, M. D. Ultrafast Two-Dimensional Infrared Vibrational Echo Chemical Exchange Experiments and Theory; *J Phys Chem B* **2006**, *110*, 19998-20013

(23) King, J. T.; Ross, M. R.; Kubarych, K. J. Water-Assisted Vibrational Relaxation of a Metal Carbonyl Complex Studied with Ultrafast 2D-IR; *J Phys Chem B* **2012**, *116*, 3754-3759

(24) Bonner, G. M.; Ridley, A. R.; Ibrahim, S. K.; Pickett, C. J.; Hunt, N. T. Probing the Effect of the Solution Environment on the Vibrational Dynamics of an Enzyme Model System with Ultrafast 2D-IR Spectroscopy; *Faraday Discussions* **2010**, *145*, 429-442

(25) Hamm, P.; Lim, M.; Hochstrasser, R. M. Vibrational Energy Relaxation of the Cyanide Ion in Water; *J Chem Phys* **1997**, *107*, 10523-10531

(26) Czurlok, D.; von Domaros, M.; Thomas, M.; Gleim, J.; Lindner, J.; Kirchner, B.; Voehringer, P. Femtosecond 2DIR Spectroscopy of the Nitrile Stretching Vibration of Thiocyanate Anions in Liquid-to-Supercritical Heavy Water. Spectral Diffusion and Libration-Induced Hydrogen-Bond Dynamics; *PhysChemChemPhys* **2015**, *17*, 29776-29785

(27) Czurlok, D.; Gleim, J.; Lindner, J.; Voehringer, P. Vibrational Energy Relaxation of Thiocyanate Ions in Liquid-to-Supercritical Light and Heavy Water. A Fermi's Golden Rule Analysis; *Journal of Physical Chemistry Letters* **2014**, *5*, 3373-3379

(28) Kim, Y. S.; Liu, L.; Axelsen, P. H.; Hochstrasser, R. M. 2D IR Provides Evidence for Mobile Water Molecules in Beta-Amyloid Fibrils; *Proc Nat Acad Sci* **2009**, *106*, 17751-17756

(29) Ghosh, A.; Qiu, J.; DeGrado, W. F.; Hochstrasser, R. M. Tidal Surge in the M2 Proton Channel, Sensed by 2D IR Spectroscopy; *Proc Nat Acad Sci* **2011**, *108*, 6115-6120

(30) Loparo, J. J.; Roberts, S. T.; Tokmakoff, A. Multidimensional Infrared Spectroscopy of Water. II. Hydrogen Bond Switching Dynamics; *J Chem Phys* **2006**, *125*, 194522

(31) Loparo, J. J.; Roberts, S. T.; Tokmakoff, A. Multidimensional Infrared Spectroscopy of Water. I. Vibrational Dynamics in Two-Dimensional IR Line Shapes; *J Chem Phys* **2006**, *125*, 194521

(32) Kraemer, D.; Cowan, M. L.; Paarmann, A.; Huse, N.; Nibbering, E. T. J.; Elsaesser, T.; Miller, R. J. D. Temperature Dependence of the Two-Dimensional Infrared Spectrum of Liquid H_2O; *Proc Nat Acad Sci* **2008**, *105*, 437-442

(33) Fenn, E. E.; Wong, D. B.; Giammanco, C. H.; Fayer, M. D. Dynamics of Water at the Interface in Reverse Micelles: Measurements of Spectral Diffusion with Two-Dimensional Infrared Vibrational Echoes; *J Phys Chem B* **2011**, *115*, 11658-11670

(34) Finkelstein, I. J.; Zheng, J. R.; Ishikawa, H.; Kim, S.; Kwak, K.; Fayer, M. D. Probing Dynamics of Complex Molecular Systems with Ultrafast 2D IR Vibrational Echo Spectroscopy; *PhysChemChemPhys* **2007**, *9*, 1533-1549

(35) Tan, H. S.; Piletic, I. R.; Riter, R. E.; Levinger, N. E.; Fayer, M. D. Dynamics of Water Confined on a Nanometer Length Scale in Reverse Micelles: Ultrafast Infrared Vibrational Echo Spectroscopy; *Phys Rev Lett* **2005**, *94*, art. no.-057405

(36) Manor, J.; Mukherjee, P.; Lin, Y.-S.; Leonov, H.; Skinner, J. L.; Zanni, M. T.; Arkin, I. T. Gating Mechanism of the Influenza A M2 Channel Revealed by 1D and 2D IR Spectroscopies; *Structure* **2009**, *17*, 247-254

(37) Mukherjee, P.; Kass, I.; Arkin, I.; Zanni, M. T. Picosecond Dynamics of a Membrane Protein Revealed by 2D IR; *Proc Nat Acad Sci* **2006**, *103*, 3528-3533

(38) Adamczyk, K.; Simpson, N.; Greetham, G. M.; Gumiero, A.; Walsh, M. A.; Towrie, M.; Parker, A. W.; Hunt, N. T. Ultrafast Infrared Spectroscopy Reveals Water-mediated Coherent Dynamics in an Enzyme Active Site; *Chemical Science* **2015**, *6*, 505-516